International Journal of Multidisciplinary Research and Development
www.allsubjectjournal.com
ISSN Online: 2349-4182 ISSN Print: 2349-5979
Received: 08-11-2025, Accepted: 07-12-2025, Published: 22-12-2025
Volume 12, Issue 12, 2025, Page No. 161-168

Flow and thermal behavior analysis in a closed enclosure filled with cu-water nanofluid considering the effect of heat conductive inner body

M U Ahammad*, Asaduzzaman Shaheen, Najmul Islam
Department of Mathematics, Dhaka University of Engineering and Technology, Gazipur, Bangladesh

Abstract
This study focuses on free convective flow and thermal behavior in a two-dimensional closed enclosure with internal heat conductive body. Under steady-state, laminar, and incompressible flow conditions, the finite element method (FEM) is used to solve the governing equations for mass, momentum, and energy conservation. The impact of important key parameters for Newtonian, water-based Cu nanofluids (Pr = 7.0), namely, the Rayleigh number ($10^4 \leq Ra \leq 10^7$) and nanoparticle volume percentage ($0.01 \leq \varphi \leq 0.1$) are analyzed in the present work. The findings are expressed by streamlines for flow patterns, isotherms for thermal distribution, and velocity as well as temperature profiles for better understanding of the considered phenomena. In addition, heat transfer rate at bottom wall is evaluated which is shown in terms of average Nusselt number. Obtained results show that heat transfer rate is higher with the increasing values of both Ra and φ; that plays a vital role for controlling the specified temperature in the studied domain.

Keywords: Free convection, closed enclosure, internal heat-conductive body, cu–water nanofluid, finite element method (FEM), Rayleigh number

Introduction

One basic method of heat transmission that is fuelled by buoyant forces resulting from density variations within a fluid is free convection, also referred to as natural convection. This phenomenon is widespread in both natural processes and a broad range of industrial applications, such as heat exchangers, solar energy systems, electronic component cooling, and building thermal management. In a variety of thermal systems where forced circulation is either unwanted or impossible, an understanding of free convective heat transfer is essential for improving energy efficiency, maximising system performance, and guaranteeing operational safety. Free convective flow and thermal behaviour in enclosed spaces are the main topics of this investigation. Closed enclosures are used in many aspects of engineering design, from food storage units and nuclear reactor insulation to double-pane windows and cabinets for electronic equipment. The intricate relationship between fluid motion and heat transmission is greatly influenced by the boundaries of such enclosures as well as certain boundary circumstances. The equilibrium between buoyant, viscosity, and thermal diffusion effects controls the complex flow patterns and temperature distributions in these small areas.

Internal heat generation within the enclosure's fluid or solid borders is a crucial factor that is frequently seen in real-world applications. Internal heat sources can be caused by phenomena including radioactive decay, exothermic chemical reactions, ohmic heating in electrical components, and metabolic activities in biological systems. Heat transfer analysis becomes more difficult and complex when internal heat production is introduced since it significantly changes the temperature and flow fields. The buoyant forces are immediately impacted by the extra energy source, which alters the convective currents and, ultimately, the system's overall thermal performance. Thus, the goal of this research is to thoroughly examine the thermal behaviour and free convective flow patterns inside a closed enclosure, taking into account the important influence of an internal heat generating parameter. The goal is to clarify the ways in which different amounts of internal heat generation affect fluid dynamics, temperature distributions, and general heat transfer properties, offering important information for the design and optimisation of systems in which these phenomena are common.

In order to improve the prediction accuracy of flow and heat transport, Qi *et al.* [1] developed a two-phase lattice Boltzmann model to mimic natural convection in composite nanofluids. Analysing nanofluid thermal behaviour in increased heat exchange systems and CPU cooling applications under magnetic fields, Fan *et al.* [5] and Qi *et al.* [6] also found better thermo-hydraulic performance. By adding magnetic and radiative effects in tilted enclosures, Aghakhani *et al.* [8] expanded on this and improved our knowledge of entropy creation in nanofluid systems. Zemani *et al.* [4] have also investigated specific nanofluids, such as CuO-water nanofluids, in U-shaped enclosures with different geometries, demonstrating that the inclusion of additional features like T-shaped baffles can further enhance natural convection and heat transfer.

The significance of nanoparticle interaction and magnetic effects on free convection is highlighted by these investigations taken together. The impact of internal heat generation on natural convection in enclosures has been assessed in a number of studies. Numerical simulations by Mahapatra and Biswal [9, 22] shown that internal heat generation has a major impact on temperature distribution and flow structure. In their investigation of nanofluid-filled porous cavities, Saleh and Hashim [10, 23] showed that heat generation amplifies buoyancy-driven circulation, changing the profiles of entropy generation and Nusselt number. In their analysis of unstable convection using the lattice Boltzmann technique, Kumar and Chamkha [11, 24] confirmed that internal heating intensifies transitory effects. MHD convection with volumetric sources was also studied by

Khan and Ahmed [12, 25], who found intricate relationships between heat sources and Lorentz forces. Internal barriers and enclosure geometry play a critical role. The effect of 2D and 3D fin designs on heat sink efficiency in magneto-hydrodynamic (MHD) systems was evaluated by Tian *et al.* [7]. In square enclosures, Billah *et al.* [16] investigated adiabatic elliptic obstructions at different points, highlighting how the position of the blockage affects the convection intensity. Azzouz & Hamida [18] examined nanohybrid fluids in variously shaped enclosures under magnetic fields, whereas Mohammed *et al.* [17] examined triangular enclosures. These changes demonstrate how enclosure form has a crucial role in determining thermal stratification and flow direction. In order to model more realistic systems, a number of works used electromagnetic effects. For instance, a thorough examination by Sheikholeslami [13, 26] shown that, depending on the field's direction and strength, the presence of a magnetic field may either stimulate or repress convection. Using a higher-order numerical method, Punia & Ray [19] examined entropy production in MHD natural convection under uniform/non-uniform heating. In order to capture fine-scale flow mechanics, sophisticated simulation methods such as Computational Fluid Dynamics (CFD) [14, 27] and the Lattice Boltzmann Method [1, 11, 24] have proved essential. In their analysis of inclined cavities with spatially changing internal heat generation, Barletta & Celli [15, 28] focused on the modulation of convective patterns by the inclination angle and the dispersion of the heat source. Similarly, Ahmed & Podder [20] assessed mixed convection in square enclosures with heated barriers, emphasising the interaction between conduction, convection, and radiation, while Kumar *et al.* [21] investigated the effect of non-gray radiation on tall cavities. A number of researchers looked at real-world systems. While Khalid *et al.* [3] concentrated on microelectronics cooling with heat pipes and nanofluids, Shahsavar *et al.* [2] investigated melting and solidification in latent heat thermal energy storage (LHTES) systems. These courses connect theoretical knowledge with practical engineering requirements.

The goal of the current study is to investigate the flow and thermal characteristics of Cu-water nanofluid inside a U-shaped cavity containing a heat conductive body. From the above-mentioned literature, it is clear that no such work has been done earlier, so this work is different based on choosing configuration, thermal state and nanofluid.

Domain Configuration

The studied domain of the present work is demonstrated in Figure 1, which is a U-shaped cavity saturated with Cu-water nanofluid. The cavity height and width are equal, and it is taken to be of length unity ($H = W = 1$). A cold rib is situated near the cavity's top; its width and depth are $l = 0.4$, $h = 0.4$ units, accordingly. An adiabatic solid body is placed inside the cavity. A temperature T_c is set at the rib, where the side walls and two upper portions of the enclosure are considered adiabatic. The bottom wall is considered heated with uniform temperature T_h. All solid boundaries are configured as no-slip walls, indicating that both u and v, the velocity elements, are nil.

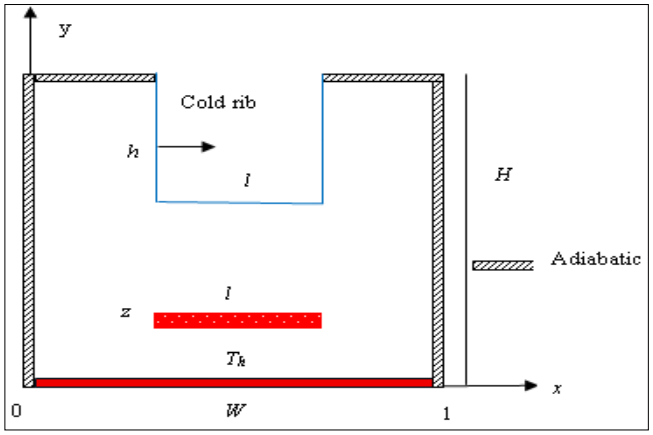

Fig 1: Studied geometry

Mathematical Formulation

The current study uses a two-dimensional, steady, laminar, Newtonian, and incompressible working fluid. The density fluctuation of the nanofluid and other thermophysical parameters are followed by the Boussinesq approximation. Table 1 displays the properties of the base fluid and the nanoparticle. Navier-Stoke's equations, which are composed of continuity, momentum, and energy equations, are used as governing equations for the problem mentioned above, which is expressed in dimensionless form below:

$$\frac{\partial U}{\partial X}+\frac{\partial V}{\partial Y}=0 \tag{1}$$

$$U\frac{\partial U}{\partial X}+V\frac{\partial U}{\partial Y}=-\frac{\partial P}{\partial X}+Pr\left(\frac{\rho_f}{\rho_{nf}}\right)\left(\frac{\mu_{nf}}{\mu_f}\right)\left(\frac{\partial^2 U}{\partial X^2}+\frac{\partial^2 U}{\partial Y^2}\right) \tag{2}$$

$$U\frac{\partial V}{\partial X}+V\frac{\partial V}{\partial Y}=-\frac{\partial P}{\partial Y}+Pr\left(\frac{\rho_f}{\rho_{nf}}\right)\left(\frac{\mu_{nf}}{\mu_f}\right)\left(\frac{\partial^2 V}{\partial X^2}+\frac{\partial^2 V}{\partial Y^2}\right)+\left(\frac{(\rho\beta)_{nf}}{\rho_{nf}\beta_f}\right)RaPr\theta \tag{3}$$

$$U\frac{\partial \theta}{\partial X}+V\frac{\partial \theta}{\partial Y}=\frac{\alpha_{nf}}{\alpha_f}\left(\frac{\partial^2 \theta}{\partial X^2}+\frac{\partial^2 \theta}{\partial Y^2}\right) \tag{4}$$

Where $Pr=\frac{\vartheta_f}{\alpha_f}$, $Ra=\frac{g\beta_f H^3(T_h-T_c)}{\vartheta_f\alpha_f}$, are the Prandtl number, and Rayleigh number respectively.

The relationships that follow are used to make equations (1) through (4) devoid of dimensions.

$$X=\frac{x}{H}, Y=\frac{y}{H}, U=\frac{uH}{\alpha_f}, V=\frac{vH}{\alpha_f}, \theta=\frac{T-T_c}{T_h-T_c}, P=\frac{pH^2}{\rho_{nf}\alpha_f^2} \tag{5}$$

Average Nusselt number at the heated wall of the enclosure is expressed as $Nu_{av}=\frac{-k_{nf}}{k_f}\int_0^1\frac{\partial\theta}{\partial X}dY$.

The boundary conditions for the problem is given below:

On the cold rib of the cavity: $U=V=0, \theta=0$

On the bottom wall of the cavity: $U=V=0, \theta=1$

On the remaining wall of the cavity and solid strip: $U=V=0, \frac{\partial\theta}{\partial N}=0$

Table 1: Copper and water's thermo-physical characteristics at 20°C

Property	Water	Copper (Cu)
$C_p(Jkg^{-1}K^{-1})$	4179	385
$\rho(kgm^{-3})$	997.1	8933
$k(Wm^{-1}K^{-1})$	0.613	401
$\beta(K^{-1})$	21×10^{-5}	1.67×10^{-5}
$\sigma(\mu S/m)$	0.05	5.96×10^{7}

Computational Procedure

The Newton-Raphson iteration technique is used to solve the designed mathematical model, which consists of equations for the conservation of mass, momentum, and energy, using a Galerkin weighted residual based FEM. The linear equations generated by the previously mentioned process will be solved in order to identify the basic unknown variables, including velocity components U, V, temperature T, and pressure P.

Grid Sensitivity Check

The problem is taken into consideration using various grid-sized elements for the highest level of accuracy. These grids measure the amount of heat removed from the two chosen sources on the enclosure's lower wall. Table 2 illustrates the minor variance in different-sized grids. Throughout the problem simulation, the grid with 21966 elements is selected.

Table 2: The Nusselt value average at the heated bottom layer when Pr = 7, $Ra = 10^4$, $\varphi = 0.05$

Number of elements	1440	2108	3295	8493	21966	28702
Nu_{av}	8.6616	9.0106	9.5596	11.312	12.725	12.728
Deviation%	-	4.03%	6.09%	18.33%	12.49%	0.024%

Code Validation

The current study's code is established by revealing a connection to Zemani *et al*.'s earlier investigation [4]. As explained below, Figure 2 illustrates the bond between these two pieces with acceptable conformity in flow and thermal fields.

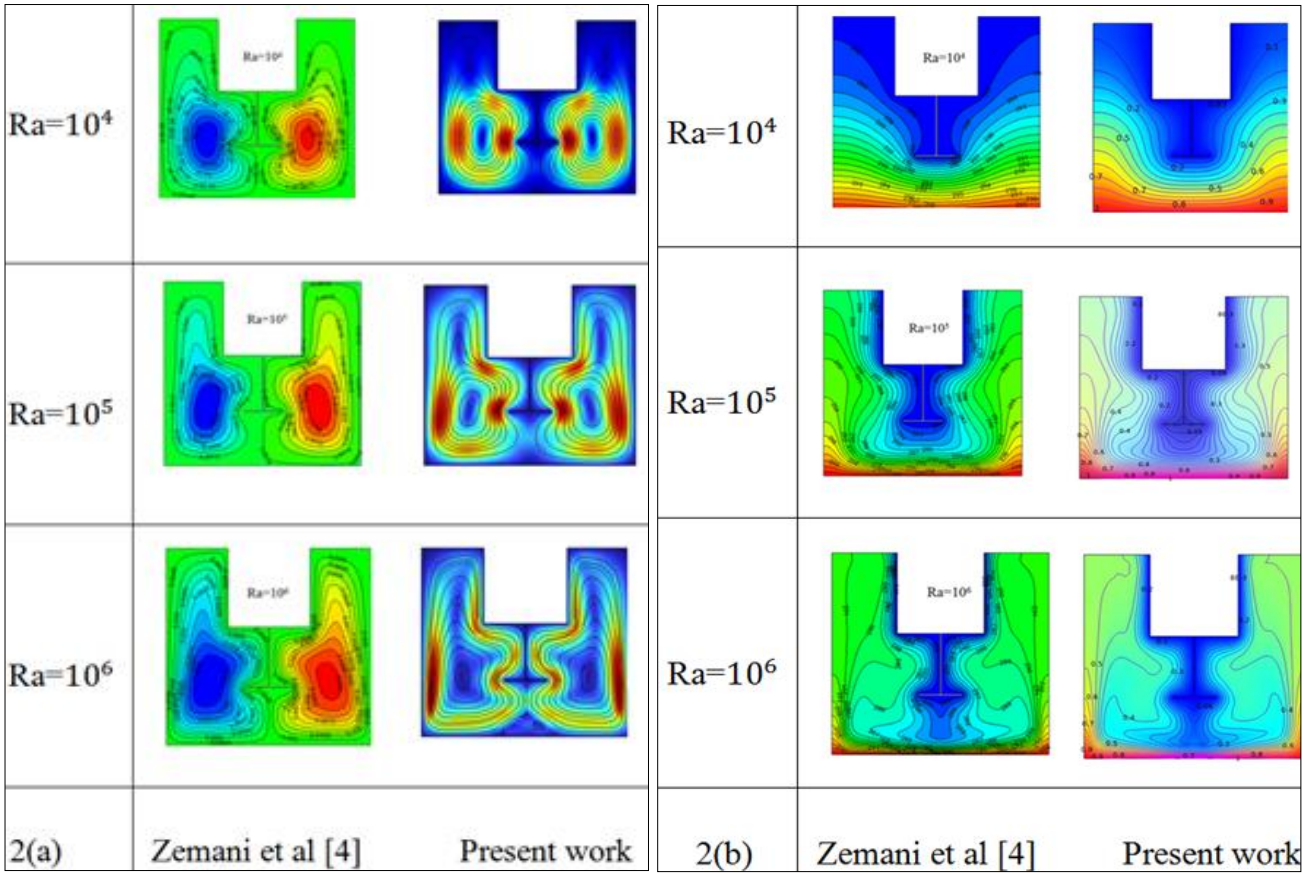

Fig 2: Comparison of (a) streamlines and (b) isotherms between the work of Zemani *et al*. [4] and present for ^{Cuo}-water nanofliud at φ = 0.05 and Pr = 7 varying Ra=$10^4 - 10^6$

Results and Discussions

The flow dynamics of a Cu-water nanofluid inside a U-shaped closed cavity with an internal heat conducting body is investigated in this study. To evaluate their impact on flow field and thermal performance, important parameters like the nanoparticle volume fraction (φ = 0.01-0.1) and Rayleigh number (Ra =10^4 - 10^7) are chosen. Understanding and controlling the Rayleigh number and nanoparticle volume fraction are crucial for many thermal systems designs and natural event research.

Effect of Rayleigh Number (*Ra*)

In fluid dynamics and heat transfer, the Rayleigh number (Ra), a dimensionless metric, is used to predict when convection will start in a fluid layer. It emphasizes the significance of the upward or downward movement brought on by variations in a liquid's density and dispersion, especially as a result of a liquid's preference. The Rayleigh number is essential for determining whether heat transfer in a fluid occurs by convection or conduction. The effects of the Ra on the heat lines and flow velocity are shown in Fig. 3. The heat lines go toward the colder area, the conduction is nearly complete, and the flow lines appear fairly uniform when the Rayleigh number, Ra, is 10^4. In Rayleigh numbers of Ra = 10^5 and Ra = 10^6, convection controls heat transmission, resulting in stronger, more

pronounced vortices. More heat is transported and buoyancy is more dominant in a more dynamic flow. The isothermal lines climb away from the vertical wall, indicating significant variations in the isotherms as well. This tendency is due to increased buoyant forces, which are associated with higher Rayleigh numbers. The buoyant force increases along with the fluid circulation strength as the Rayleigh number rises. As a result, heat transmission is improved as the liquid transfers' warmth more effectively from the heated area to the cool area. For larger Rayleigh numbers, Ra = 10^7, conductive heat transmission reduces as Ra increases. Stronger streamline circulation patterns and more complex isothermal distributions result from the takeover of convection.

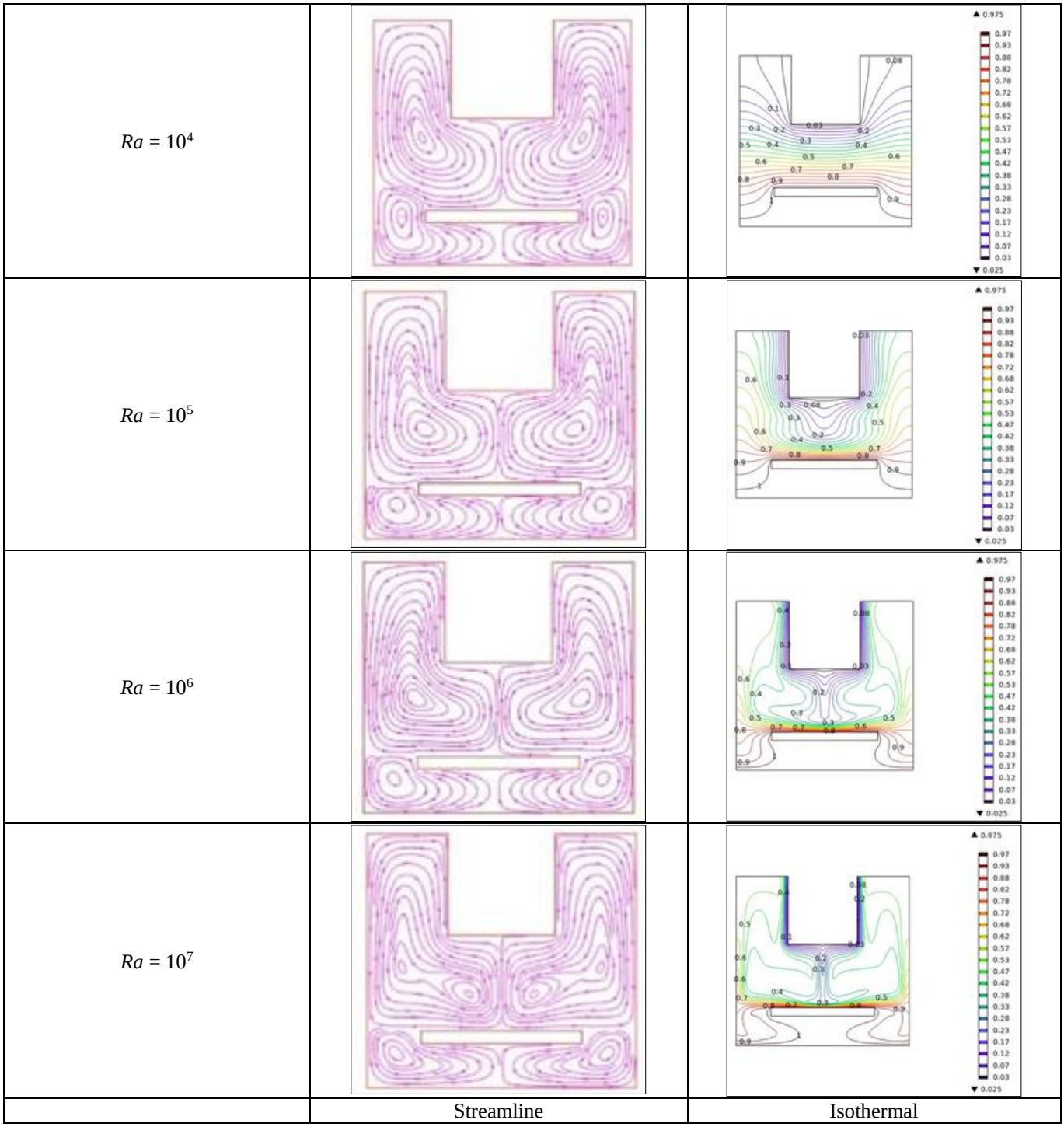

Fig 3: Streamlines and isotherms for the variation of *Ra*

Figures 4(a), (b), and (c) show the effects of Ra = 10^4–10^7 on the velocity, temperature, and temperature gradient magnitude profiles. Where the vertical line's y axix component of the velocity field ranges from -1200 to 800 in (a) and the horizontal line's pressure magnitude ranges from 0 to 1. The temperature profile is shown in Figure (b), where the vertical line for Ra change varies between 0.2 and 0.75. In particular, figure (c) shows the arc length (0 to 1) on the horizontal line and the variation of Ra for the heat gradient (k/m) value of (0 to 6.5) on the vertical line.

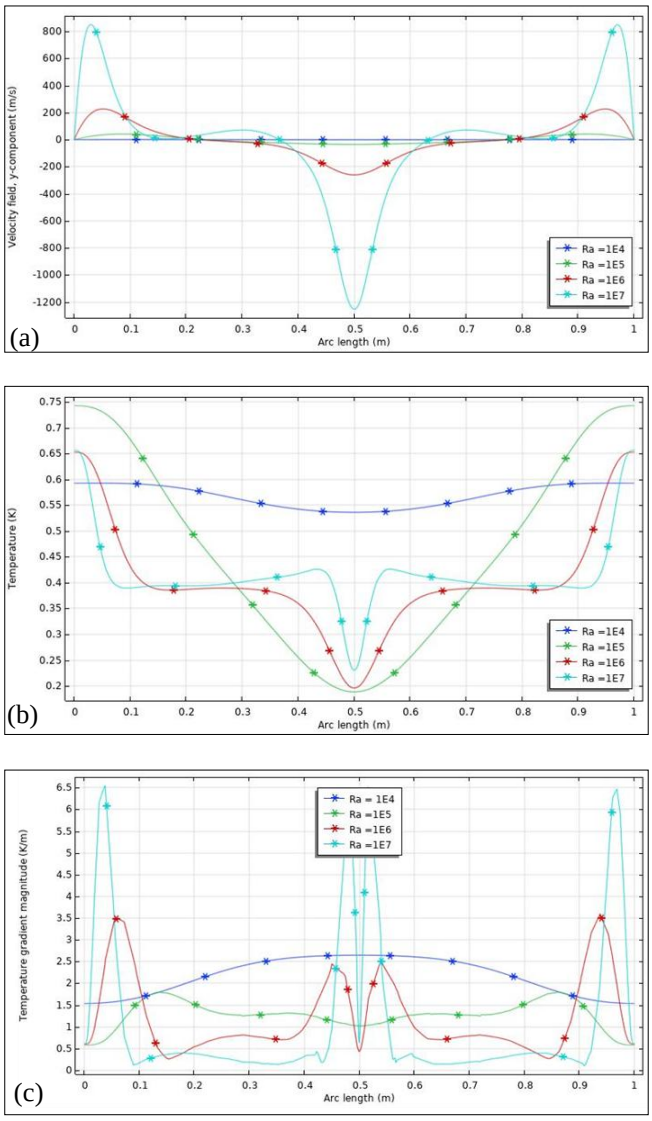

Fig 4: (a) Velocity profile, (b) temperature, for the variation of Ra

Table 3: The Nusselt value average near the wall of heat for various Ra levels when Pr =7 and φ = 0.05

Ra	10^4	10^5	10^6	10^7
Nu_{av}	1.3318	2.9879	6.2332	11.193

The Nu_{av} at the heated wall for different *Ra* is shown in Table 3 while maintaining a constant Prandtl number (Pr) of 7 and a ϕ of 0.05. The table demonstrates a trend: the Nu_{av} rises in tandem with the *Ra*. This suggests that under these particular circumstances, heat dispersion from the heated wall becomes more effective at larger *Ra*. For the constant values of Pr and ϕ, these data points indicate a direct correlation between the efficiency of heat transmission (represented by Nu_{av}) and the strength of natural convection (represented by *Ra*).

Effect of nanoparticle volume fraction (φ)

The impact of nanoparticle volume fraction on streamlines and isotherms is shown in Fig.5. At φ = 0.1, the streamlines reach their maximum intensity, exhibiting distinct vortex patterns, strong circulation, and isotherm lines that get closer to the cold groove. Streamlines grow more intense, nanoparticles increase heat conductivity, which enhances circulation and heat transfer, and the isotherms exhibit noticeable variations at φ = 0.05 and φ = 0.08. The isothermal lines along the vertical wall alter and become more concentrated, indicating increased heat convection. This suggests that buoyancy-driven flow has a greater effect, increasing the system's ability to transmit heat. These phenomena are caused by the higher buoyant forces that accompany a lower volume fraction. As it descends, buoyant forces rise and the fluid circulates more vigorously. Improved heat transfer may allow the fluid to transfer heat from the hot surface to the cold surface more efficiently. For φ = 0.01, the streamlines are relatively weak, indicating a reduced convective impact. When the fluid velocity stays sluggish and the isotherm lines center in the ground portion of the hole near the heat source, it indicates a high-temperature zone. At higher levels (such as φ = 0.1), conductive heat transmission is lower than at lower values (such as φ = 0.01). When it falls from φ = 0.1 to φ = 0.01, convection takes precedence, leading to more intricate isothermal patterns and increased fluid circulation in the streamlines. In contrast, the isothermal contours display the distribution of heat and temperature fluctuations.

The streamlined shapes display the kind and strength of convecting currents, while the isothermal contours depict the distribution of heat and temperature changes. These findings demonstrate the dynamic interaction between convective and conductive heat transfer processes and the crucial role that buoyant forces play in defining the thermal behavior of nanofluids.

φ = 0.01	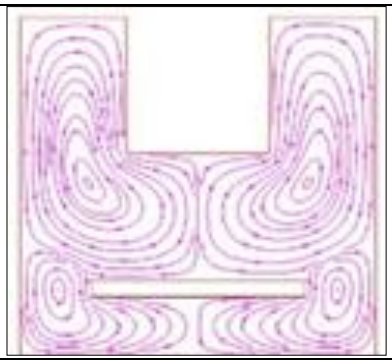	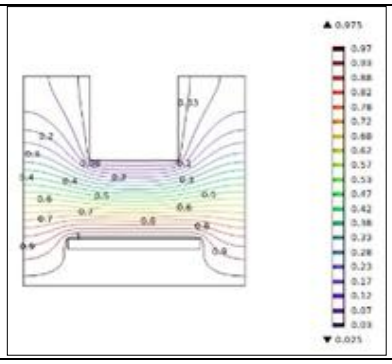

φ = 0.05	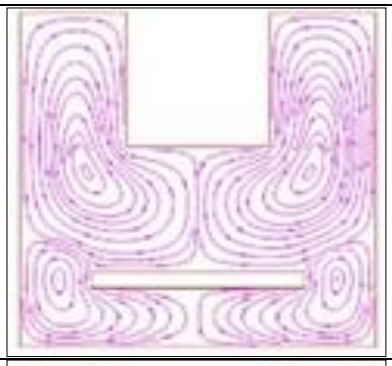	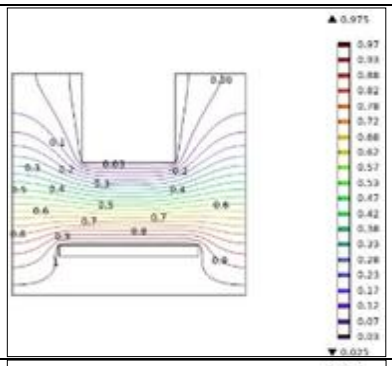
φ = 0.08	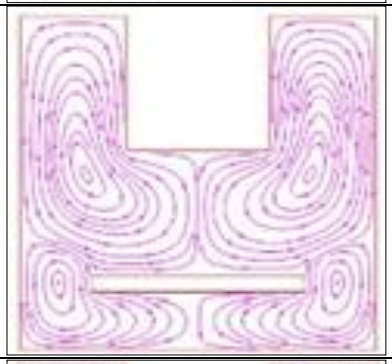	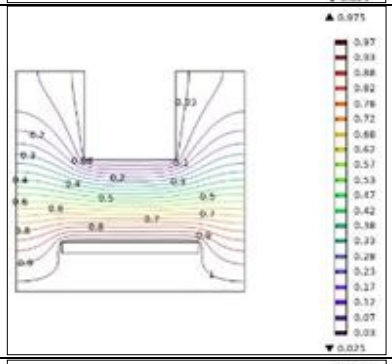
φ = 0.1	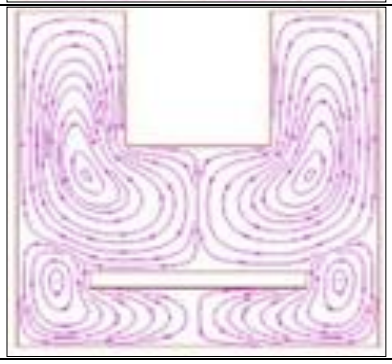	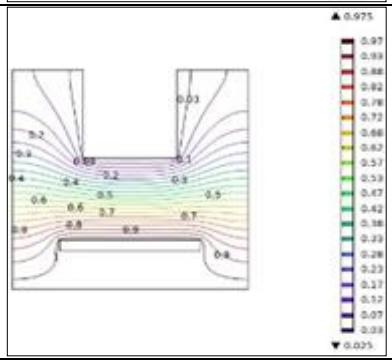
	Streamlines	Isotherms

Fig 5: Streamlines and Isotherms with varying nanoparticle volume fraction φ

Figures 6 (a), (b), and (c) illustrate the effects of φ = 0.01–0.1 through velocity, temperature, and temperature gradient profile. The arc length of the horizontal line runs from 0 to 1, but the velocity field y-component (m/s) of the vertical line spans from -1200 to 800. When φ changes in (b), the temperature (0.2 to 0.75) rises and dips along the vertical line. Lastly, it is evident that the variation of φ = 0.01-0.1 in (c), where the temperature gradient magnitude (k/m) is 0 to 6.5 in

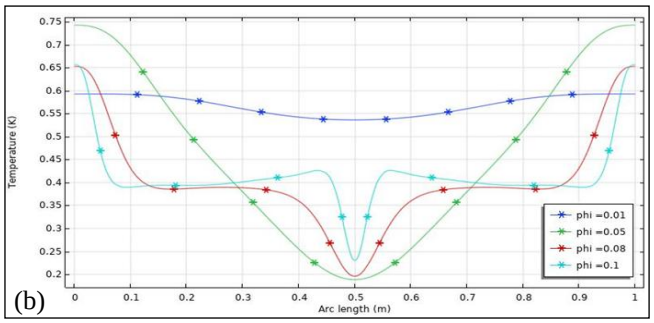

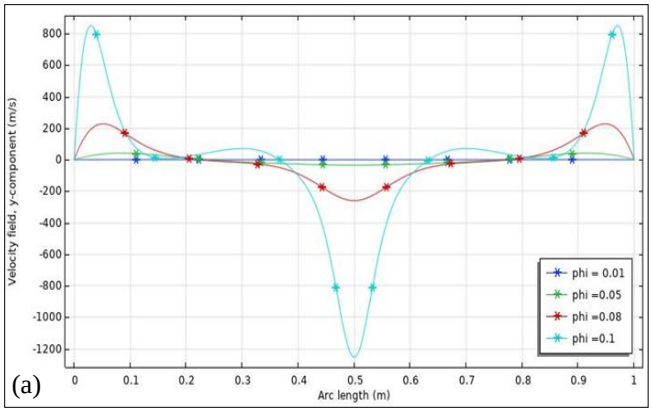

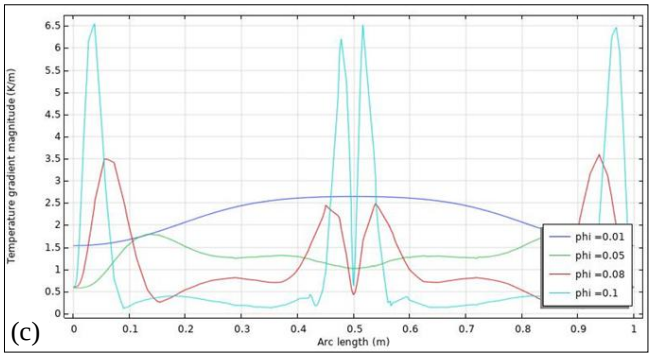

Fig 6: For the fluctuation of φ, (a) velocity profile, (b) temperature profile, and (c) gradient of temperature profile

Table 4: Average Nusselt value for various values at a warmed surface of φ when Pr =7 and $Ra = 10^4$

φ	0.01	0.05	0.08	0.1
Nu_{av}	0.19068	0.21652	0.23696	0.25120

The table 4 shows the average Nusselt value at bottom heated wall temperature values for the different values φ. The data's parameters are set at a Rayleigh number (*Ra)* of 10^4 and a Prandtl number (Pr) of 7, which are common for fluid systems with modest natural convection, including water-based nanofluids. The Nu_{av} rises in tandem with various φ values. This suggests that a larger concentration of nanoparticles improves convective heat transfer efficacy. From 0.19068 (φ = 0.01) to 0.25120 (φ = 0.1), Nu_{av} increased, indicating a notable improvement in heat transmission capabilities.

Conclusion

By including the impact of the internal heat conducting body, the current study concentrated on the free convective flow and thermal behavior in a closed enclosure. The results of the analysis showed that the flow structure and temperature distribution are considerably changed by inner body within the enclosure. The major outcomes of this work can be summarized as follows:

- Free convective parameter Ra affects the temperature distribution inside the cavity sharply.
- More heat transfer rate is found for the higher values of Ra.
- A minor change is followed in flow pattern and thermal behavior with the rising values of nanoparticle volume concentration.
- As φ increases, heat removal performance is higher.

References

1. Qi C, Tang J, Wang G. Natural convection of composite nanofluids based on a two-phase lattice Boltzmann model. Journal of Thermal Analysis and Calorimetry,2020:141:277–287.
2. Shahsavar A, Ali HM, Mahani RB, Talebizadehsardari P. Numerical study of melting and solidification in a wavy double-pipe latent heat thermal energy storage system. Journal of Thermal Analysis and Calorimetry, 2020.
3. Khalid SU, Babar H, Ali HM, Janjua MM, Ali MA. Heat pipes: progress in thermal performance enhancement for microelectronics. Journal of Thermal Analysis and Calorimetry, 2020.
4. Farah Zemani, Omar Ladjedel, Amina Sabeur. Simulation of CuO-water nanofluid natural convection in a U-shaped enclosure with a T-shaped baffle. Journal of Engineering and Applied Science,2023:70:99. https://doi.org/10.1186/s44147-023-00257-x
5. Fan F, Qi C, Tang J, Liu Q, Wang X, Yan Y. A novel thermal efficiency analysis on the thermo-hydraulic performance of nanofluids in an improved heat exchange system under adjustable magnetic field. Applied Thermal Engineering,2020:179:115688.
6. Qi C, Tang J, Fan F, Yan Y. Effects of magnetic field on thermo-hydraulic behaviors of magnetic nanofluids in CPU cooling system. Applied Thermal Engineering,2020:179:115717.
7. Tian MW, Rostami S, Aghakhani S, Goldanlou AS, Qi C. Investigation of 2D and 3D configurations of fins and their effects on heat sink efficiency of MHD hybrid nanofluid with slip and non-slip flow. International Journal of Mechanical Sciences, 2020, 105975.
8. Aghakhani S, Pordanjani AH, Afrand M, Sharifpur M, Meyer JP. Natural convective heat transfer and entropy generation of alumina/water nanofluid in a tilted enclosure with an elliptic constant temperature: applying magnetic field and radiation effects. International Journal of Mechanical Sciences,2020:174:105470.
9. Mahapatra TR, Biswal S. Natural convection in a square enclosure with internal heat generation: a numerical study. International Journal of Heat and Mass Transfer,2022:193:123024.
10. Saleh H, Hashim I. Effect of internal heat generation on natural convection in a porous cavity filled with nanofluid. Alexandria Engineering Journal,2021:60(5):4879–4891.
11. Kumar A, Chamkha AJ. Unsteady natural convection in an enclosure with heat generation using lattice Boltzmann method. Journal of Thermal Analysis and Calorimetry,2023:143:1237–1252.
12. Khan WA, Ahmed S. Numerical study of MHD natural convection in a square cavity with volumetric heat sources. Case Studies in Thermal Engineering,2020:18:100586.
13. Sheikholeslami M. Heat transfer behavior of nanofluids in enclosures under the influence of internal heat generation and magnetic field: a comprehensive review. Renewable and Sustainable Energy Reviews,2023:176:113189.
14. Huang H, Deng Q. Thermal performance of a differentially heated cavity with internal heat sources using CFD. Applied Thermal Engineering,2021:190:116802.
15. Barletta A, Celli M. Natural convection in inclined cavities with spatially varying internal heat generation. International Journal of Heat and Fluid Flow,2022:95:108920.
16. Billah SS, Hossain MS, Asad MF, Mallik MSI, Paul SC, Munshi MJH, *et al*. Free convection at different locations of adiabatic elliptic blockage in a square enclosure. Mathematical Modelling and Numerical Simulation with Applications,2024:4(1):86–109.
17. Mohammed AA, Mohammed AA, Channapattanac SV. Experimental investigation into natural convection heat transfer inside triangular enclosure with internal hot cylinder. Al-Nahrain Journal for Engineering Sciences,2023:26(3):175–185.
18. Azzouz R, Hamida MB. Natural convection in two different enclosures filled with nanohybrid under magnetic field: application to heat exchanger. Thermal Science,2025:2025(1):114.
19. Punia A, Ray RK. Effect of uniform and non-uniform wall heating on three-dimensional magneto-hydrodynamics natural convection and entropy generation: a computational study using new higher order super compact scheme. arXiv preprint,2024:2408:01853.
20. Ahmed H, Podder C. Mixed convection heat transfer and flow of Al_2O_3-water nanofluid in a square enclosure

with heated obstacles and varied boundary conditions. arXiv preprint,2024:2401:05497.
21. Kumar P, Chanakya G, Barthwal N. Investigations of non-gray/gray radiative heat transfer effect on natural convection in tall cavities at low operating temperature. arXiv preprint,2020:2011:03709.
22. Mohapatra TR, Biswal S. Natural convection in a square enclosure with internal heat generation: a numerical study. International Journal of Heat and Mass Transfer,2022:193:123024.
23. Saleh H, Hashim I. Effect of internal heat generation on natural convection in a porous cavity filled with nanofluid. Alexandria Engineering Journal,2021:60(5):4879–4891.
24. Kumar A, Chamkha AJ. Unsteady natural convection in an enclosure with heat generation using lattice Boltzmann method. Journal of Thermal Analysis and Calorimetry,2023:143:1237–1252.
25. Khan WA, Ahmed S. Numerical study of MHD natural convection in a square cavity with volumetric heat sources. Case Studies in Thermal Engineering,2020:18:100586.
26. Sheikholeslami M. Heat transfer behavior of nanofluids in enclosures under the influence of internal heat generation and magnetic field: a comprehensive review. Renewable and Sustainable Energy Reviews,2023:176:113189.
27. Huang H, Deng Q. Thermal performance of a differentially heated cavity with internal heat sources using CFD. Applied Thermal Engineering,2021:190:116802.
28. Barletta A, Celli M. Natural convection in inclined cavities with spatially varying internal heat generation. International Journal of Heat and Fluid Flow,2022:95:108920.